

# **Optimization of High-Pressure Vapor-Liquid Equilibrium Modelling of Binary Mixtures (Supercritical Fluid + Ionic Liquid) by Particle Swarm Algorithm**

**Juan A. Lazzús\***

*Departamento de Física, Universidad de La Serena, Casilla 554, La Serena, Chile*

*jlazzus@dfuls.cl*

(Received December 13, 2014)

## **Abstract**

High-pressure vapor–liquid equilibrium data of binary mixtures containing supercritical fluids and imidazolium ionic liquids were correlated using a thermodynamic model optimized with a particle swarm algorithm. The Peng–Robinson (PR) equation of state and the Wong–Sandler (WS) mixing rules including the van Laar (VL) model for the excess Gibbs free energy, were used as thermodynamic model. Forty six binary systems taken from literature were selected for this study, and the optimization algorithm was used to determine the binary interaction parameters of each system. The algorithm was development to minimize the difference between calculated and experimental bubble pressure. The results given by the model show that the proposed algorithm is a good tool to correlate and describe the vapor–liquid equilibrium of this type of systems.

## **1. Introduction**

In the recent years, room temperature ionic liquids (RTILs) or just ionic liquids (ILs) came into focus because of their potential as alternatives for several engineering applications [1]. ILs are typically composed of a large organic cation and an inorganic polyatomic anion.

There is virtually no limit in the number of possible ionic liquids since there is a large number of cations and anions that can be combined [2]. At ambient room temperature, they exist as liquids and have a wide variety of unique properties (for instance, negligible vapor pressure, favorable chemical behavior, low viscosity, and high reactivity and selectivity) [3]. The most commonly used cation in room-temperature ionic liquids (RILs) is dialkylimidazolium. And in recent years, 1-*alkyl*-3-methylimidazolium ( $[C_n\text{mim}]^+$ ) ILs have been intensively studied [1].

The increasing utilization of ILs in chemical and industrial processes requires reliable and systematic thermophysical properties such as activity coefficients, heats of mixing, densities, solubilities, vapor–liquid equilibria (VLE), and liquid–liquid equilibria (LLE). In addition, the transport properties are also needed (viscosity, electric conductivity, mutual diffusion coefficients, etc.) [4]. For a better understanding of their thermodynamic behavior and for the development of thermodynamic models reliable experimental phase equilibrium data is required [5]. Phase equilibrium data of mixtures containing ionic liquids are necessary for further development of some separation processes involving supercritical fluids. Blanchard et al. [6] described several potential applications of supercritical fluids with ILs. They demonstrated the possibility of using supercritical carbon dioxide ( $\text{CO}_2$ ) to remove a solute from an IL, without contamination of the extracted solute, solving one of the shortcomings of the use of ionic liquids in solvent extraction processes: the recovery of the compounds from the ionic liquid media [7]. Scurto et al. [8] proposed an innovative process of separating ILs from organic solvents using supercritical  $\text{CO}_2$  that induces a phase separation, due to the organic liquid phase expansion and the dielectric constant decrease, forcing the IL to separate into a second liquid phase [7]. Later, Scurto et al. [9] also demonstrated that separation of aqueous solutions of both hydrophobic and hydrophilic ILs can be performed using supercritical  $\text{CO}_2$  [7]. The solubility of carbon dioxide in a variety of ILs has been determined at low pressures and high pressures [10]. The gas solubilities data provides important information for the characterization of solute-solvent interactions and so contribute to understand the mechanisms of dissolution. From a practical point of view, gas solubility can be useful in the calculation of vapor-liquid equilibrium (VLE) [11].

On this line, VLE data for binary systems including ionic liquids, although essential for the design and operation of separation processes, are still scarce. Recently, some works have presented binary VLE data involving several ionic liquids and such organic compounds as alkanes, alkenes and aromatics, as well as supercritical fluids [12]. Various models have been used to correlate experimental data of phase equilibria of these systems [13]. One of the

common approaches used in the literature to correlate and predict phase equilibrium requires an equation of state that well relates the variables temperature, pressure and volume and appropriate mixing rules to express the dependence of the equation of state parameters on the concentration [14]. On equations of state, the Peng–Robinson equation has been used to describe the solubility of ILs in supercritical fluids [15].

The existing methods to solve phase equilibrium systems give only local solutions. It has been demonstrated that for cases of systems containing supercritical CO<sub>2</sub>, the optimum values of the interaction parameters depend on the searching interval and on the initial value of used interaction parameters [16].

Parameter estimation procedures are very important in engineering, industrial, and chemical process for development of mathematical models, since design, optimization and advanced control of bioprocesses depend on model parameter values obtained from experimental data. The aim of optimization is to determine the best-suited solution to a problem under a given set of constraints. Mathematically, an optimization problem involves a fitness function describing the problem, under a set of constraints representing the solution space for the problem. The optimization problem, now-a-days, is represented as an intelligent search problem, where one or more agents are employed to determine the optimum on a search landscape [17]. Modern optimization techniques have aroused great interest among the scientific and technical community in a wide variety of fields recently, because of their ability to solve problems with non-linear and non-convex dependence of design parameters [18]. Thus, the use of heuristic optimization methods, such particle swarm optimization (PSO) [19], for the parameter estimation is very promising [20]. This biologically-derived method represents an excellent alternative to find a global optimum for phase equilibrium calculations [14-18].

In this work, forty-six binary vapor-liquid phase systems containing supercritical fluids (CO<sub>2</sub> or CHF<sub>3</sub>) + 1-*alkyl*-3-methylimidazolium ILs were correlated using a thermodynamic model optimized with a PSO algorithm. The Peng–Robinson (PR) equation of state and the Wong–Sandler (WS) mixing rules including the van Laar (VL) model for the excess Gibbs free energy were used as thermodynamic model. The algorithm was developed to calculate the binary interaction parameters, and used for minimize the difference between calculated and experimental bubble pressure.

## 2. Particle swarm optimization

Adjustable parameters are a common feature of most thermodynamic models for phase equilibrium calculations. Most of the existing methods for solving phase equilibrium and stability problems are local in nature and at best yield only local solutions. Use of global techniques in these problems is relatively unexplored and deserves greater investigation [21]. Because of the difficulties in evaluating the first derivatives, to locate the optima for many rough and discontinuous optimization surfaces, in recent times, several derivative algorithms have emerged [20]. Particle swarm optimization (PSO) is a relatively recently devised population-based stochastic global optimization algorithm. As described by Eberhart and Kennedy, the PSO algorithm is an adaptive algorithm based on a social-psychological metaphor; a population of individuals (referred to as particles) adapts by returning stochastically toward previously successful regions [19].

The PSO algorithm is initialized with a population of random particles and the algorithm searches for optima by updating generations [22]. In a PSO system, each particle is “flown” through the multidimensional search space, adjusting its position in search space according to its own experience and that of neighboring particles. The particle therefore makes use of the best position encountered by itself and that of its neighbors to position itself toward an optimal solution [23]. The performance of each particle is evaluated using a predefined fitness function, which encapsulates the characteristics of the optimization problem [24].

Each particle is associated with velocity that indicates where the particle is traveling. Let  $k$  be a time instant. The new particle position is computed by adding the velocity vector to the current position

$$s_{k+1}^i = s_k^i + v_{k+1}^i \quad (1)$$

when  $s$  and  $v$  denote a particle position and its corresponding velocity in a search space, respectively. Being  $s_k^i$  particle  $i$  position,  $i = 1, \dots, \rho$ , at time instant  $k$ ,  $v_{k+1}^i$  new velocity (at time  $k+1$ ) and  $\rho$  is population size.

The velocity update equation is given by:

$$v_{k+1}^i = w_k v_k^i + c_1 r_1 (p_k^i - s_k^i) + c_2 r_2 (p_k^g - s_k^i) \quad (2)$$

where  $k$  is the current step number,  $w$  is the inertia weight,  $c_1$  and  $c_2$  are the acceleration constants, and  $r_1, r_2$  are element from two random sequences in the range  $[0, 1]$ . The current position of the particle is determined by  $s_k^i$ ;  $p_k^i$  is the best one of the solutions this particle has reached,  $p_k^g$  is the best one of the solutions all the particles have reached [22].

The variable  $w$  [25] is responsible for dynamically adjusting the velocity of the particles, so it is responsible for balancing between local and global search, hence requiring fewer iterations for the algorithm to converge. A low value of inertia weight implies a local search, while a high value leads to a global search. Applying a large inertia weight at the start of the algorithm and making it decay to a small value through the PSO execution makes the algorithm search globally at the beginning of the search, and search locally at the end of the execution [23]. The following weighting function  $w$  is used in Eq. (2):

$$w = w_{max} - \frac{w_{max} - w_{min}}{k_{max}} k \tag{3}$$

Generally, the value of each component in  $v$  can be clamped to the range  $[-v_{max}, v_{max}]$  control excessive roaming of particles outside the search space [17]. After calculating the velocity, the PSO algorithm performs repeated applications of the update equations above until a specified number of iteration has been exceeded, or until the velocity updates are close to zero [23]. The PSO algorithm is presented in detail in Table 1. Figure 1 shows the update systems of the PSO algorithm. Figure 2 shows the flow diagram of the PSO algorithm used.

In PSO, the inertial weight  $w$ , the constant  $c_1$  and  $c_2$ , the number of particles  $N_{part}$  and the maximum speed of particle summarize the parameters to synchronize for their application in a given problem. An exhaustive trial-and-error procedure was applied for tuning the PSO parameters. Firstly, the effect of  $w$  was analyzed for values from 0.1 to 0.9. Figure 3a shows the values of  $w$  that favored the search of the particles and accelerated the convergence. Next, the effect of  $N_{part}$  was analyzed for values from 100 to 1000 particles in the swarm. Figure 3b

**Table 1.** Scheme of the PSO algorithm development in this study.

Step	Description
1	Initialize algorithm: population size and number of weights and biases. Set constants: $k_{max}, v_{max}, w, c_1, c_2$
2	Randomly initialize the swarm positions $s_0^i \in \mathbb{R}^n$ for $i = 1, \dots, \rho$
3	Randomly initialize particle velocities $v_0^i$ for $i = 1, \dots, \rho$
4	Set $k = 1$ Evaluate function value $F_k^i$ using design space coordinates $s_k^i$ :
5	If $F_k^i \leq F_{best}^i$ then $F_{best}^i = F_k^i, p_k^i = s_k^i$ If $F_k^i \leq F_{best}^g$ then $F_{best}^g = F_k^i, p_k^g = s_k^i$
6	If stopping condition is satisfied then stop algorithm
7	Update all particle velocities $v_k^i$ for $i = 1, \dots, \rho$
8	Update all particle positions $s_k^i$ for $i = 1, \dots, \rho$
9	Otherwise set $k = k + 1$ goes to step 5

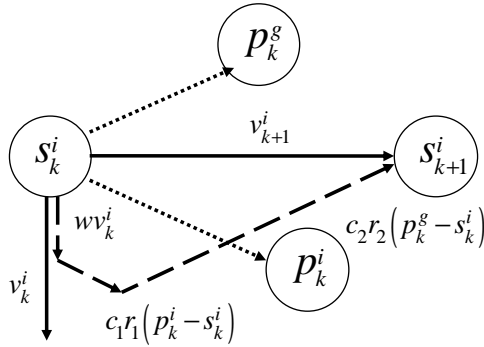


**Figure 1.** PSO position and velocity update.

shows that the best population to solve the problem is of 25 particles. Table 2 shows the selected parameters for the PSO algorithm.

### 3. Equations of vapor–liquid equilibrium

As known, the phase equilibrium problem to be solved consists of the calculation of some variables of the set  $T$ – $P$ – $x$ – $y$  (temperature, pressure, liquid–phase concentration and vapor–phase concentration, respectively), when some of them are known. For a vapor–liquid mixture in thermodynamic equilibrium, the temperature and the pressure are the same in both phases, and the remaining variables are defined by the material balance and the “*fundamental equation of phase equilibrium*” [26]. The application of this fundamental equation requires the use of thermodynamic models which normally include binary interaction parameters. These binary parameters must be determined using experimental data for binary systems. Theoretically, once these binary parameters are known one could predict the behavior of multicomponent mixtures using standard thermodynamic relations and thermodynamics models [27].

The fundamental equation of vapor–liquid equilibrium can be expressed as the equality of fugacities of each component in the mixture in both phases [26]:

$$\bar{f}_i^L = \bar{f}_i^V \quad (4)$$

where the superscripts  $L$  and  $V$  represent liquid and vapor, respectively.

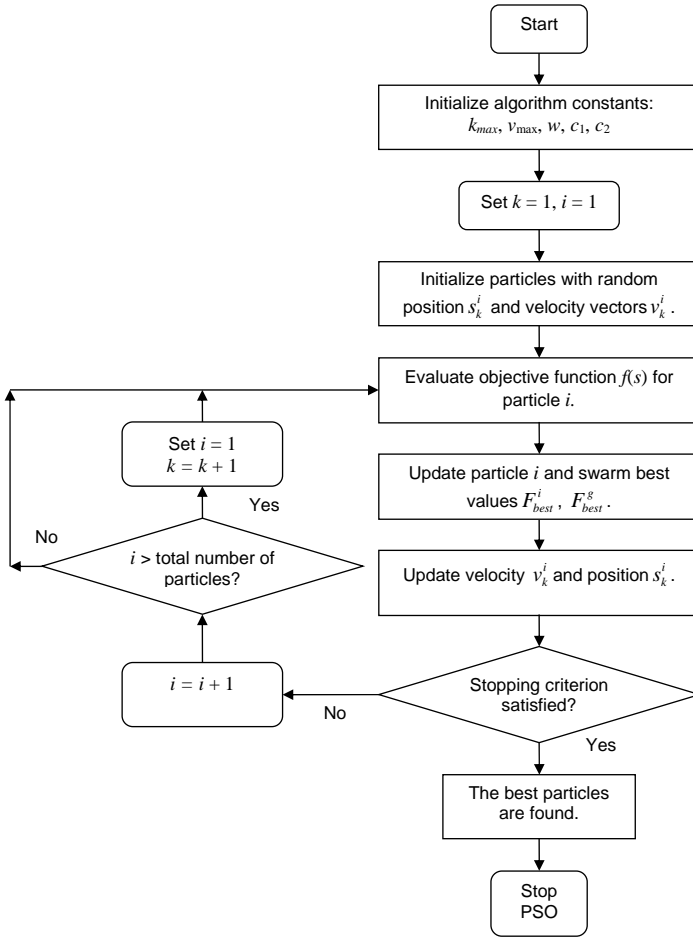


**Figure 2.** Flow diagram of the PSO algorithm used in this study.

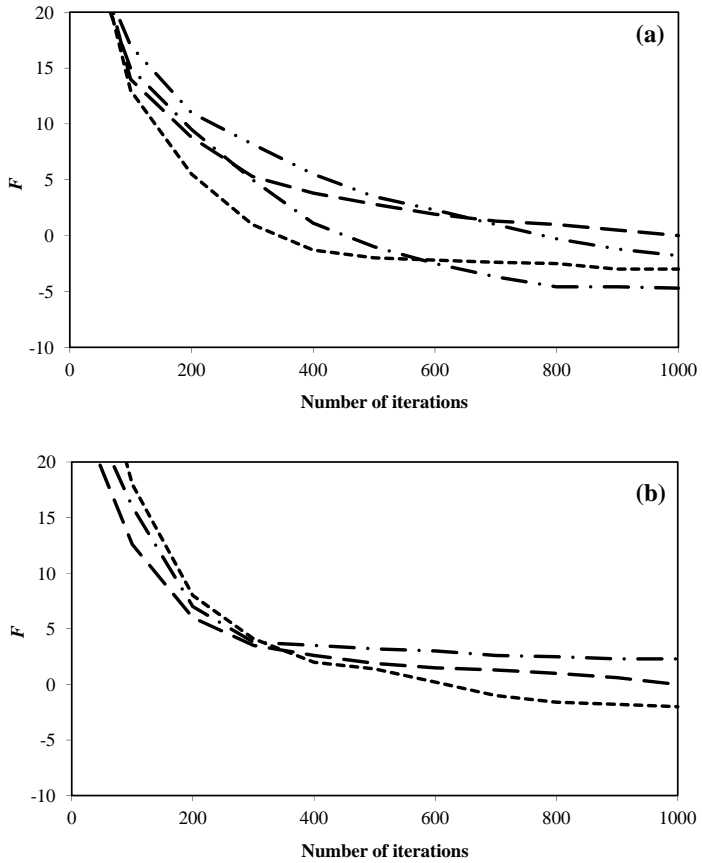


**Figure 3.** Convergence graphics. (a) Determination of the best values for  $w$  as: 0.3(—), 0.5(- - -), 0.7(- · - ·), 0.9 (- · · · - ·). (b) Effect of  $N_{part}$  for: 25(- - -), 50(—), 100(- · · - ·).

**Table 2.** Parameters used in the PSO algorithm.

PSO Parameter	Value
Number of particles in swarm ( $N_{part}$ )	25
Number of iterations ( $k_{max}$ )	1000
Cognitive component ( $c_1$ )	1.494
Social component ( $c_2$ )	1.494
Maximum velocity ( $v_{max}$ )	12
Minimum inertia weight ( $w_{min}$ )	0.5
Maximum inertia weight ( $w_{max}$ )	0.7

The fugacity of a component in the vapor phase is usually expressed through the fugacity coefficient  $\bar{\phi}^V$  :

$$\bar{f}_i^V = y_i \bar{\phi}_i^V P \quad (5)$$

And the fugacity of a component in the liquid phase is expressed through either the fugacity coefficient  $\bar{\phi}^L$  or the activity coefficient  $\gamma_i$  :

$$\bar{f}_i^L = x_i \bar{\phi}_i^L P \quad (6)$$

$$\bar{f}_i^L = x_i \gamma_i f_i^0 \quad (7)$$

In these equations,  $y_i$  is the mole fraction of component in the vapor phase,  $x_i$  is the mole fraction of component in the liquid phase, and  $P$  is the pressure. The fugacity is related to the temperature, the pressure, the volume and the concentration through a standard thermodynamic relation [28].

If the fugacity coefficient is used in both phases, the method of solution of the phase equilibrium problem is known as “*the equation of state method*”. Then, equation of state (EoS) and a set of mixing rules are needed to express the fugacity coefficient as function of the temperature, the pressure and the concentration [26]. Modern EoS methods include an excess Gibbs free energy model ( $G^E$ ) in the mixing rules of the EoS, giving origin to the so-called “*equation of state +  $G^E$  model*” [27]. This means that an activity coefficient model ( $\gamma$ ) is used to describe the complex liquid phase, and the fugacity coefficient ( $\phi$ ) is calculated using a simple equation of state. If the fugacity coefficient is used for the vapor phase and the activity coefficient is used for the liquid phase the equilibrium problem is known as “*the gamma-phi method*” ( $\gamma$ - $\phi$ ) [26].

#### 4. Equation of state method

From the relation between the fugacity, the Gibbs free energy, and an EoS, the fugacity in a vapor can be calculated as:

$$\ln \left[ \frac{\bar{f}_i^V(T, P, y_i)}{y_i P} \right] = \ln \bar{\phi}_i \quad (8)$$

$$\ln \bar{\phi}_i = \frac{1}{RT} \int_{V=\infty}^V \left[ \frac{RT}{V} - \left( \frac{\partial P}{\partial N_i} \right)_{T, V, N_{i \neq j}} \right] dV - \ln Z^V \quad (9)$$

where  $V$  is the total volume, and  $Z = PV \underline{(RT)}^{-1}$  is the compressibility factor calculated from as EoS, and  $\underline{V}$  is the molar volume of the mixture [27].

The most common EoS used for the correlation of phase equilibria in mixtures at high and low pressure are the cubic equations derived from van der Waals EoS [29]; among these, the Peng–Robinson equation has proven to combine the simplicity and accuracy required for the prediction and correlation of volumetric and thermodynamic properties of fluids [30].

The Peng–Robinson EoS was expressed as follows [30]:

$$P = \frac{RT}{\underline{V} - b} + \frac{a}{\underline{V}(\underline{V} + b) + b(\underline{V} - b)} \quad (10)$$

with

$$a = 0.457235 \frac{R^2 T_c^2}{P_c} \alpha(T_r) \quad (11)$$

$$b = 0.077796 \frac{RT_c}{P_c} \quad (12)$$

$$\alpha(T_r) = \left[ 1 + \kappa \left( 1 - \sqrt{T_r} \right) \right]^2 \quad (13)$$

$$\kappa = 0.37646 + 1.54226\omega - 0.26992\omega^2 \quad (14)$$

where  $Tr = T/T_c$  is the reduced temperature. In this form, the Peng–Robinson EoS is completely predictive once the constants (critical temperature  $T_c$ , critical pressure  $P_c$ , and acentric factor  $\omega$ ) are given. Consequently, this equation is a two-parameter EoS ( $a$  and  $b$ ) that depends upon the three constants ( $T_c$ ,  $P_c$ , and  $\omega$ ) [27].

For mixtures, the parameters  $a$  and  $b$  are expressed as functions of the concentration of the different components in the mixture, through the so-called mixing rules [26]. Until recent years, most of the applications of EoS to mixtures considered the use of the classical van der

Waals mixing rules, with the inclusion of an interaction parameter for the force constant  $a$  and volume constant  $b$ . The Peng–Robinson EoS for a mixture is:

$$P = \frac{RT}{\underline{V} - b_m} + \frac{a_m}{\underline{V}(\underline{V} + b_m) + b_m(\underline{V} - b_m)} \quad (15)$$

The classical van der Waals mixing rules are [27]:

$$a_m = \sum_i \sum_j x_i x_j a_{ij} \quad (16)$$

$$b_m = \sum_i \sum_j x_i x_j b_{ij} \quad (17)$$

and the combining rules for  $a_{ij}$  and  $b_{ij}$ , with interaction parameters for the force and volume constants, are:

$$a_{ij} = \sqrt{a_i a_j} (1 - k_{ij}) \quad (18)$$

$$b_{ij} = \frac{b_i + b_j}{2} (1 - l_{ij}) \quad (19)$$

The parameters  $k_{ij}$  and  $l_{ij}$  in the above combining rules for the equation of state are usually calculated by regression analysis of experimental phase equilibrium data.

The modern equation of state includes an excess Gibbs free energy model in the mixing rules of the EoS. Thus, the connection between equations of state + excess Gibbs free energy, seem to be the most appropriate for modeling complex mixtures [29].

The Wong–Sandler mixing rule is an example of these types of mixing rules, and can be summarized as follows [31]:

$$b_m = \frac{\sum_i \sum_j x_i x_j \left( b - \frac{a}{RT} \right)_{ij}}{1 - \sum_i \frac{x_i a_i}{b_i RT} - \frac{A_\infty^E(x)}{\Omega RT}} \quad (20)$$

$$\left( b - \frac{a}{RT} \right)_{ij} = \frac{1}{2} (b_i + b_j) - \frac{\sqrt{a_i a_j}}{RT} (1 - k_{ij}) \quad (21)$$

$$a_m = b_m \left( \sum_i \frac{x_i a_i}{b_i} + \frac{A_\infty^E(x)}{\Omega} \right) \quad (22)$$

In these equations  $a_m$  and  $b_m$  are the equation of state constants with  $k_{ij}$  as adjustable parameter,  $\Omega=0.34657$  for the PR EoS, and  $A_\infty^E(x)$  is calculated assuming that  $A_\infty^E(x) \approx A_0^E(x) \approx G_0^E(x)$ .

For a binary mixture:

$$b_m = \frac{x_1^2 \left( b - \frac{a}{RT} \right)_1 + 2x_1x_2 \left( b - \frac{a}{RT} \right)_{12} + x_2^2 \left( b - \frac{a}{RT} \right)_2}{1 - \frac{x_1a_1}{b_1RT} - \frac{x_2a_2}{b_2RT} - \frac{G_0^E(x)}{\Omega RT}} \quad (23)$$

$$\left( b - \frac{a}{RT} \right)_{12} = \frac{1}{2}(b_1 + b_2) - \frac{\sqrt{a_1a_2}}{RT} (1 - k_{12}) \quad (24)$$

$$a_m = b_m \left( \frac{x_1a_1}{b_1RT} + \frac{x_2a_2}{b_2RT} + \frac{G_0^E(x)}{\Omega} \right) \quad (25)$$

The excess Gibbs free energy  $G_0^E(x)$  in the mixing rules is calculated using an appropriate liquid-phase model. In this work,  $G_0^E(x)$  has been calculated using the van Laar model that has been shown to perform well in high pressure phase equilibrium calculations [15].

The van Laar model for  $G_0^E(x)$  is described by the following equation [26]:

$$\frac{G_0^E}{RT} = \sum_i x_i \frac{\sum_j x_j A_{ij}}{1 - x_j} \left[ 1 - \frac{x_i \sum_j x_j A_{ij}}{x_i \sum_j x_j A_{ij} + (1 - x_i) x_i \sum_j x_j A_{ij}} \right]^2 \quad (26)$$

For a binary mixture, the model reduces to:

$$\frac{G_0^E}{RT} = \frac{A_{12}x_1x_2}{x_1 \left( \frac{A_{12}}{A_{21}} \right) + x_2} \quad (27)$$

Thus, the problem is reduced here to determine the interaction parameters  $A_{12}$ ,  $A_{21}$ , and the  $k_{12}$  parameter included in the combining thermodynamic model (PR-WS-VL), using available high pressure  $T$ - $P$ - $x$  data of vapor-liquid phase equilibrium of complex mixtures. These optimal interaction parameters were determined by minimizing the following objective function in data regression, using a hybrid algorithm based on particle swarm optimization and ant colony optimization:

$$\min F = \frac{100}{N_D} \sum_{i=1}^{N_D} \left| \frac{P^{calc} - P^{exp}}{P^{exp}} \right| \quad (28)$$

where  $N_D$  is the number of points in the experimental data set and  $P$  is the pressure of the ionic liquid in the vapor phase, the superscript denotes the experimental (*exp*) data point and calculated (*calc*) values. Figure 4 shows the flow diagram of the total algorithm development for the vapor–liquid equilibrium modeling.

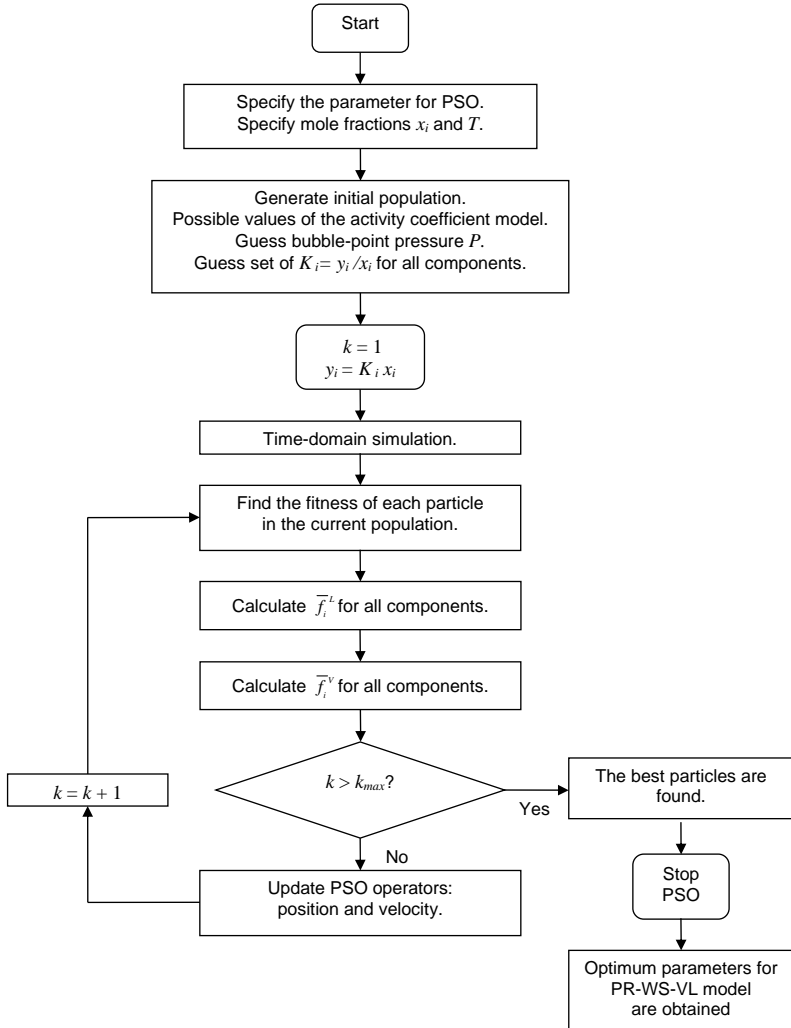
Forty-six binary vapor–liquid phase systems containing supercritical carbon dioxide and imidazolium-based ionic liquids were considered in this study. The anions: bis(trifluoromethylsulfonyl)imide ([Tf<sub>2</sub>N]), hexafluorophosphate ([PF<sub>6</sub>]), tetrafluoroborate ([BF<sub>4</sub>]), ethyl sulfate ([EtSO<sub>4</sub>]), dicyanamide ([DCA]), nitrate ([NO<sub>3</sub>]), trifluoromethanesulfonate ([TfO]), and tris(trifluoromethylsulfonyl)methide ([methide]), are the ones presenting the highest supercritical carbon dioxide solubility. Although both anion and cation influence the carbon dioxide solubility, the anion has the strongest influence [32]. And the most common 1-*alkyl*-3-methylimidazolium cations were used: 1-ethyl-3-methylimidazolium ([C<sub>2</sub>mim]), 1-butyl-3-methylimidazolium ([C<sub>4</sub>mim]), 1-pentyl-3-methylimidazolium ([C<sub>5</sub>mim]), 1-hexyl-3-methylimidazolium ([C<sub>6</sub>mim]), and 1-octyl-3-methylimidazolium ([C<sub>8</sub>mim]).

Table 3 shows the thermodynamic properties of the substances involved in the study. In this Table,  $T_c$  is the critical temperature,  $P_c$  is the critical pressure, and  $\omega$  is the acentric factor. The data for the ionic liquids were taken from the literature [33]. The data for supercritical fluids were taken from Daubert *et al* [34]. The details of the experimental vapor–liquid equilibrium data taken from references [35-40] are presented in Table 4. As seen in the Table, the temperature and pressure ranges are narrow and go from 313K to 333K and from 0 to 43 MPa, respectively.

## 5. Results and discussion

The PR-WS-VL model and the PSO algorithm were used to calculate  $k_{12}$ ,  $A_{12}$  and  $A_{21}$ , and  $P$  by minimizing the Eq. (28), and considering the absolute deviations between experimental and calculated values of bubble point in the vapor–liquid phase of the ionic liquids on the supercritical carbon dioxide. In order to provide a substantial margin of safety, the range for the interaction parameters ( $A_{12}$  and  $A_{21}$  for VL model for the excess Gibbs free energy) was defined as  $[-5, 5]$ . This wide range was based on physical considerations [27], and is extremely likely that it will contain the optimal parameter values. In addition, the range for the WS parameter  $k_{12}$  with theoretical bases [31] was defined as  $[-1, 1]$ . Figure 5 shows

the interaction parameters determined with the proposed algorithm and based on the minimization



**Figure 4.** Flow diagram of the total algorithm used for the vapor–liquid equilibrium modeling.**Table 3.** Thermodynamic properties of the substances involved in this study.

Substance	$T_c$ (K)	$P_c$ (MPa)	$\omega$
[C <sub>2</sub> mim][Tf <sub>2</sub> N]	1214.2	3.37	0.2818
[C <sub>4</sub> mim][Tf <sub>2</sub> N]	1265.0	2.76	0.2656
[C <sub>5</sub> mim][Tf <sub>2</sub> N]	1249.4	2.63	0.4123
[C <sub>6</sub> mim][Tf <sub>2</sub> N]	1287.3	2.39	0.3539
[C <sub>8</sub> mim][Tf <sub>2</sub> N]	1311.9	2.10	0.4453
[C <sub>4</sub> mim][PF <sub>6</sub> ]	708.9	1.73	0.7553
[C <sub>8</sub> mim][PF <sub>6</sub> ]	800.1	1.40	0.9069
[C <sub>4</sub> mim][BF <sub>4</sub> ]	632.3	2.04	0.8489
[C <sub>8</sub> mim][BF <sub>4</sub> ]	726.1	1.60	0.9954
[C <sub>2</sub> mim][EtSO <sub>4</sub> ]	1061.1	40.40	0.3368
[C <sub>4</sub> mim][DCA]	1035.8	2.44	0.8419
[C <sub>4</sub> mim][NO <sub>3</sub> ]	946.3	2.73	0.6000
[C <sub>4</sub> mim][TfO]	1158.0	2.90	0.4118
[C <sub>4</sub> mim][methide]	1571.4	2.40	0.1320
CO <sub>2</sub>	304.2	7.38	0.2236
CHF <sub>3</sub>	299.30	4.79	0.2640

of bubble pressure. These results show that the pressures of the ionic liquids in the vapor phase were correlated with low deviations between experimental and calculated values (deviations are below 4%). Results of the modeling are presented in Tables 5 to 7. Table 5 shows the optimum values and deviations calculated for the binary interaction parameters  $k_{12}$ ,  $A_{12}$  and  $A_{21}$  at 313K (19 systems). Table 6 shows the optimum values and deviations calculated for the binary interaction parameters  $k_{12}$ ,  $A_{12}$  and  $A_{21}$  at 323K (8 systems). Table 7 shows the optimum values and deviations calculated for the binary interaction parameters  $k_{12}$ ,  $A_{12}$  and  $A_{21}$  at 333K (19 systems). From the results contained in these Tables, it is possible to determine the capability of the algorithm to correlate the experimental data according to the anion type: [Tf<sub>2</sub>N] (1.5%) ~ [methide] (1.5%) < [PF<sub>6</sub>] (2.0%) < [EtSO<sub>4</sub>] (2.2%) < [NO<sub>3</sub>] (2.4%) < [DCA] (2.8%) < [BF<sub>4</sub>] (2.9%) < [TfO] (3.7%). And for the case of cation type: [C<sub>3</sub>mim] (1.5%) < [C<sub>2</sub>mim] (1.6%) ~ [C<sub>6</sub>mim] (1.6%) < [C<sub>8</sub>mim] (2.0%) < [C<sub>4</sub>mim] (2.4%). One reason for the better results is the election of the thermodynamic model selected. In particular the parameters of the van Laar model included in the Wong–Sandler mixing rules. Among the many cubic EoS of van der Waals type nowadays available, the one proposed by Peng–Robinson EoS is widely used because of its simplicity and flexibility [27]. This equation has proven to combine the simplicity and accuracy required for the prediction and correlation of fluid

properties, in particular of phase equilibria [30,31]. The effect of the uncertainty of the critical properties in the phase equilibria calculations using PR-EoS has been investigated for several

**Table 4.** Details on the phase equilibrium data of all systems used in this study.

Component (1)	Component (2)	<i>T</i> (K)	$\Delta x_{SCF}$	$\Delta P$ (MPa)	Ref
CHF <sub>3</sub>	[C <sub>2</sub> mim][PF <sub>6</sub> ]	313	0.5–1.0	5–22	[35]
	[C <sub>4</sub> mim][PF <sub>6</sub> ]	323	0.1–0.8	1–18	[36]
CO <sub>2</sub>	[C <sub>2</sub> mim][Tf <sub>2</sub> N]	313	0.2–0.8	1–28	[37]
		323	0.2–0.8	1–34	
		333	0.2–0.8	2–39	
	[C <sub>4</sub> mim][Tf <sub>2</sub> N]	313	0.3–0.8	2–13	[38]
		333	0.2–0.6	1–10	
		333	0.2–0.7	2–13	
	[C <sub>8</sub> mim][Tf <sub>2</sub> N]	313	0.2–0.8	1–27	[37]
		323	0.2–0.8	1–38	
		333	0.2–0.8	2–43	
	[C <sub>4</sub> mim][Tf <sub>2</sub> N]	333	0.0–0.7	0–10	[39]
		313	0.3–0.7	1–10	[38]
		313	0.3–0.8	2–12	
		333	0.2–0.7	2–11	
	[C <sub>8</sub> mim][Tf <sub>2</sub> N]	313	0.3–0.8	1–11	[38]
		333	0.2–0.8	2–11	
	[C <sub>4</sub> mim][NO <sub>3</sub> ]	313	0.2–0.5	2–9	[39]
		323	0.2–0.5	2–9	
		333	0.2–0.5	2–9	
		313	0.1–0.5	1–9	[38]
		333	0.1–0.4	1–9	
	[C <sub>4</sub> mim][PF <sub>6</sub> ]	313	0.0–0.7	0–10	[39]
		323	0.0–0.7	0–9	
		333	0.0–0.7	0–9	
		313	0.3–0.7	2–15	[38]
		333	0.2–0.5	2–12	
		313	0.0–0.6	0–10	[40]
		333	0.0–0.5	0–9	
	[C <sub>8</sub> mim][PF <sub>6</sub> ]	313	0.0–0.8	0–9	[39]
		323	0.0–0.7	0–9	
		333	0.0–0.7	0–9	
	[C <sub>4</sub> mim][BF <sub>4</sub> ]	313	0.1–0.5	1–8	[38]
		333	0.1–0.4	1–9	
	[C <sub>8</sub> mim][BF <sub>4</sub> ]	313	0.0–0.7	0–9	[39]
	323	0.0–0.7	0–9		
	333	0.0–0.7	0–9		
[C <sub>4</sub> mim][DCA]	313	0.2–0.6	1–10	[38]	
	333	0.2–0.5	2–11		
[C <sub>4</sub> mim][TfO]	313	0.1–0.6	1–9	[38]	
	333	0.1–0.5	2–10		
[C <sub>2</sub> mim][EtSO <sub>4</sub> ]	313	0.0–0.4	0–9	[39]	
	323	0.0–0.4	0–9		
	333	0.0–0.5	0–9		
[C <sub>4</sub> mim][methide]	313	0.3–0.8	2–11	[38]	
	333	0.3–0.7	2–11		

systems, but the general trend and curvature of the phase equilibrium curve is not altered [41]. The interaction parameters represent the functionality of the constants of the equation with the concentration. It has been recognized that van der Waals mixing rules with one or two

parameters do not give good results for systems complex [42]. The Wong–Sandler mixing rules have shown to be successful in these applications. In other works to improve the

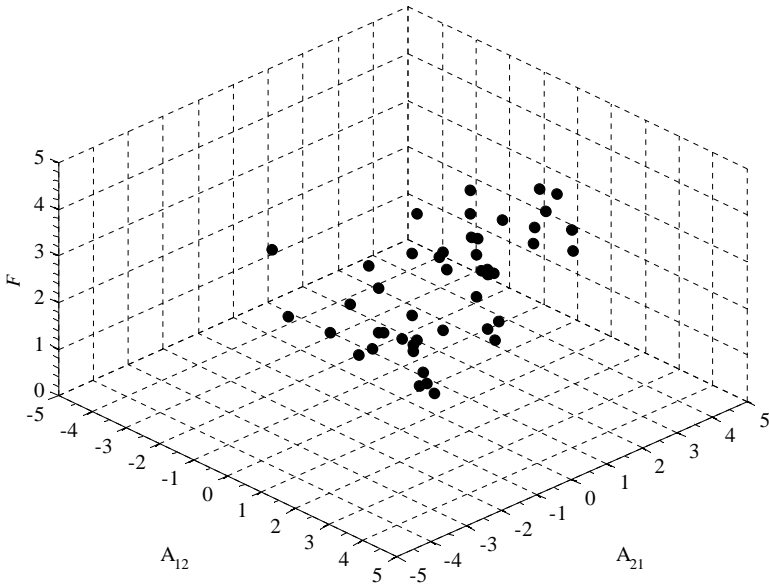


**Figure 5.** Deviations of the binary interaction parameters estimated by minimization of the objective function with PSO algorithm.

predictions in mixtures, a third interaction parameter has been introduced and has been shown that these mixing rules allow an accurate representation that when the van der Waals mixing rules are used [29]. Figure 6 shows the variation of the binary interaction parameters as a function of the absolute temperature. It can be observed the behavior of the parameters included in the PR-WS-VL model. The parameter  $k_{12}$  decreases with the temperature in most of the cases studied. For the mixing rules, parameter  $A_{12}$  shows a smooth behavior, and  $A_{21}$  shows a dynamical behavior. This is not unusual in complex systems and in particular in mixtures containing ionic liquids. Figure 7 shows the inner behavior among the parameters. The different influence of the parameters and their range of variation provide the PR-WS-VL

model greater flexibility in the sense that the model can better capture the different behavior of the mixtures studied.

**Table 5.** Optimum values and deviations calculated for the interaction parameters at 313K.

No.	Comp. (1)	Comp. (2)	$N_D$	$k_{12}$	$A_{12}$	$A_{21}$	$F$
1	CO <sub>2</sub>	[C <sub>2</sub> mim][Tf <sub>2</sub> N]	9	0.022507	1.373719	-0.432528	0.7
2	CO <sub>2</sub>	[C <sub>4</sub> mim][Tf <sub>2</sub> N]	8	0.328208	-0.208918	-0.343116	1.5
3	CO <sub>2</sub>	[C <sub>5</sub> mim][Tf <sub>2</sub> N]	9	0.051633	0.485197	-0.172968	1.4
4	CO <sub>2</sub>	[C <sub>6</sub> mim][Tf <sub>2</sub> N]	6	0.286430	-0.573135	-0.314959	1.0
5	CO <sub>2</sub>	[C <sub>6</sub> mim][Tf <sub>2</sub> N]	8	0.306212	-1.616238	-0.520215	1.0
6	CO <sub>2</sub>	[C <sub>8</sub> mim][Tf <sub>2</sub> N]	8	0.287135	-0.277280	-0.429227	1.5
7	CO <sub>2</sub>	[C <sub>4</sub> mim][NO <sub>3</sub> ]	15	0.580020	0.170878	2.091295	2.1
8	CO <sub>2</sub>	[C <sub>4</sub> mim][NO <sub>3</sub> ]	6	0.453010	0.554586	2.300081	3.3
9	CO <sub>2</sub>	[C <sub>4</sub> mim][PF <sub>6</sub> ]	8	0.263818	0.597590	4.271429	2.0
10	CO <sub>2</sub>	[C <sub>4</sub> mim][PF <sub>6</sub> ]	7	0.411644	0.329473	1.794402	2.6
11	CO <sub>2</sub>	[C <sub>4</sub> mim][PF <sub>6</sub> ]	7	0.574130	0.346160	0.064369	1.4
12	CO <sub>2</sub>	[C <sub>8</sub> mim][PF <sub>6</sub> ]	8	0.520032	0.702086	2.060538	1.2
13	CO <sub>2</sub>	[C <sub>4</sub> mim][BF <sub>4</sub> ]	8	0.711712	0.416026	1.542849	3.1
14	CO <sub>2</sub>	[C <sub>8</sub> mim][BF <sub>4</sub> ]	15	0.246681	0.566494	3.368683	3.6
15	CO <sub>2</sub>	[C <sub>4</sub> mim][DCA]	8	0.561975	0.072210	0.209615	3.1
16	CO <sub>2</sub>	[C <sub>4</sub> mim][TfO]	8	0.261265	0.243863	1.683275	3.4
17	CO <sub>2</sub>	[C <sub>2</sub> mim][EtSO <sub>4</sub> ]	7	0.246364	0.633591	1.485990	1.9
18	CO <sub>2</sub>	[C <sub>4</sub> mim][methide]	8	0.453328	-3.706182	-0.148095	2.0
19	CHF <sub>3</sub>	[C <sub>2</sub> mim][PF <sub>6</sub> ]	9	0.425688	1.887282	0.801336	1.7

**Table 6.** Optimum values and deviations calculated for the interaction parameters at 323K.

No.	Comp. (1)	Comp. (2)	$N_D$	$k_{12}$	$A_{12}$	$A_{21}$	$F$
1	CO <sub>2</sub>	[C <sub>2</sub> mim][Tf <sub>2</sub> N]	9	0.013064	1.136329	-0.400236	0.9
2	CO <sub>2</sub>	[C <sub>3</sub> mim][Tf <sub>2</sub> N]	9	0.039546	0.424277	-0.149092	2.0
3	CO <sub>2</sub>	[C <sub>4</sub> mim][NO <sub>3</sub> ]	15	0.446882	0.098396	3.982439	2.7
4	CO <sub>2</sub>	[C <sub>4</sub> mim][PF <sub>6</sub> ]	8	0.297458	0.403482	4.425513	2.3
5	CO <sub>2</sub>	[C <sub>8</sub> mim][PF <sub>6</sub> ]	9	0.442001	0.483123	2.148675	2.2
6	CO <sub>2</sub>	[C <sub>8</sub> mim][BF <sub>4</sub> ]	15	0.233528	0.520944	3.910373	3.3
7	CO <sub>2</sub>	[C <sub>2</sub> mim][EtSO <sub>4</sub> ]	7	0.178948	0.462659	1.980020	2.3
8	CHF <sub>3</sub>	[C <sub>4</sub> mim][PF <sub>6</sub> ]	12	0.439714	-0.468050	0.841052	3.5

**Table 7.** Optimum values and deviations calculated for the interaction parameters at 333K.

No.	Comp. (1)	Comp. (2)	$N_D$	$k_{12}$	$A_{12}$	$A_{21}$	$F$
1	CO <sub>2</sub>	[C <sub>2</sub> mim][Tf <sub>2</sub> N]	9	0.006276	0.996485	-0.375292	1.0
2	CO <sub>2</sub>	[C <sub>4</sub> mim][Tf <sub>2</sub> N]	6	0.194922	-0.387085	-0.321831	2.4
3	CO <sub>2</sub>	[C <sub>4</sub> mim][Tf <sub>2</sub> N]	8	0.220644	-1.030649	-0.518951	1.8
4	CO <sub>2</sub>	[C <sub>5</sub> mim][Tf <sub>2</sub> N]	9	0.028576	0.450108	-0.138636	1.2
5	CO <sub>2</sub>	[C <sub>6</sub> mim][Tf <sub>2</sub> N]	7	0.443719	0.568007	0.592748	3.1
6	CO <sub>2</sub>	[C <sub>6</sub> mim][Tf <sub>2</sub> N]	8	0.176286	-0.017627	-0.005778	1.3
7	CO <sub>2</sub>	[C <sub>8</sub> mim][Tf <sub>2</sub> N]	8	0.225224	-0.494772	-0.774673	1.0
8	CO <sub>2</sub>	[C <sub>4</sub> mim][NO <sub>3</sub> ]	15	0.426896	0.022651	2.126675	2.7
9	CO <sub>2</sub>	[C <sub>4</sub> mim][NO <sub>3</sub> ]	6	0.014869	0.837501	1.609614	1.3
10	CO <sub>2</sub>	[C <sub>4</sub> mim][PF <sub>6</sub> ]	8	0.341022	0.223758	3.535592	2.6
11	CO <sub>2</sub>	[C <sub>4</sub> mim][PF <sub>6</sub> ]	7	0.488527	0.310290	0.742218	2.9
12	CO <sub>2</sub>	[C <sub>4</sub> mim][PF <sub>6</sub> ]	10	0.620025	0.443629	0.040391	0.4
13	CO <sub>2</sub>	[C <sub>8</sub> mim][PF <sub>6</sub> ]	8	0.414298	0.384503	0.792178	1.3
14	CO <sub>2</sub>	[C <sub>4</sub> mim][BF <sub>4</sub> ]	7	0.444785	0.891908	2.868427	2.7
15	CO <sub>2</sub>	[C <sub>8</sub> mim][BF <sub>4</sub> ]	15	0.451623	0.281490	2.145473	2.0
16	CO <sub>2</sub>	[C <sub>4</sub> mim][DCA]	8	0.599104	-0.977082	-0.028139	2.5
17	CO <sub>2</sub>	[C <sub>4</sub> mim][TfO]	7	0.111228	0.256481	1.682555	4.0
18	CO <sub>2</sub>	[C <sub>2</sub> mim][EtSO <sub>4</sub> ]	7	0.151572	0.121284	1.154691	2.4
19	CO <sub>2</sub>	[C <sub>4</sub> mim][methide]	8	0.339021	-2.837799	-0.520582	1.0

A comparison was made between of the results obtained with the PSO algorithm and results obtained with Levenberg–Marquart algorithm (LM). Note that, LM [43] is commonly used in these problems. Figure 8 shows the average pressure deviations found with PSO and LM for all ionic liquids considered in this study. As is observed in the figures, the best method to estimate the vapor–liquid equilibrium of the systems used is the PSO algorithm.

Thus, the results show that the application of PSO algorithm on thermodynamic model (PR-WS-VL), was crucial, and that the proposed algorithm is a good tool to optimize the interaction parameters to describe the vapor–liquid equilibrium of several systems containing supercritical fluids and ionic liquids at high-pressures.

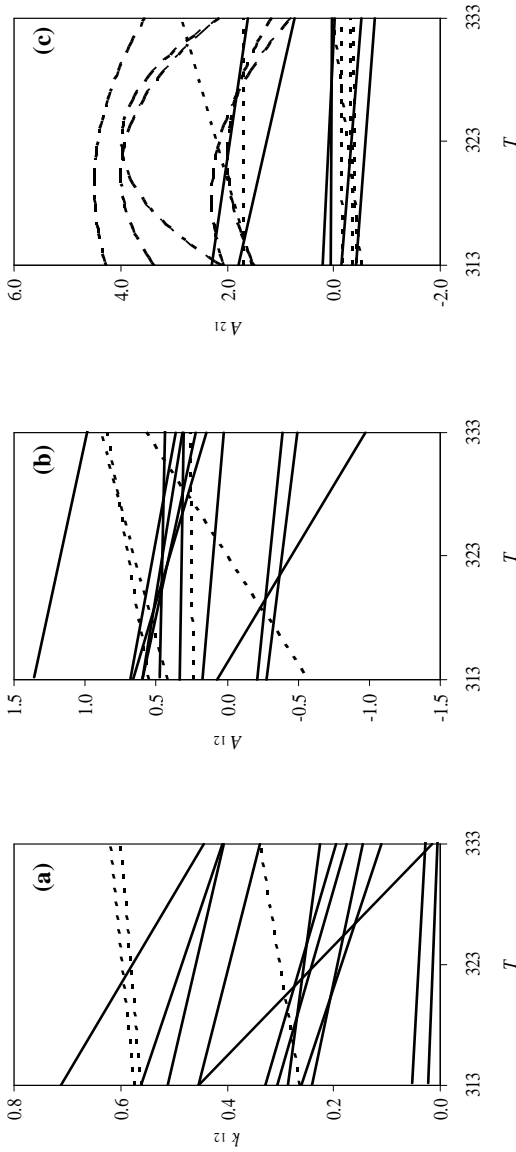


**Figure 6.** Variation of the binary interaction parameters as a function of the absolute temperature. (a) Wong-Sandler parameter  $k_{12}$ , (b) van Laar parameter  $A_{12}$ , (c) van Laar parameter  $A_{21}$ .

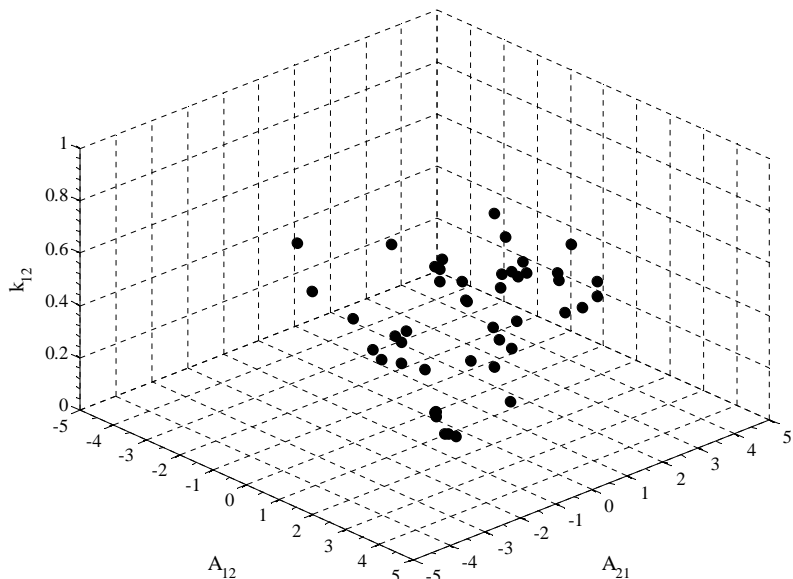
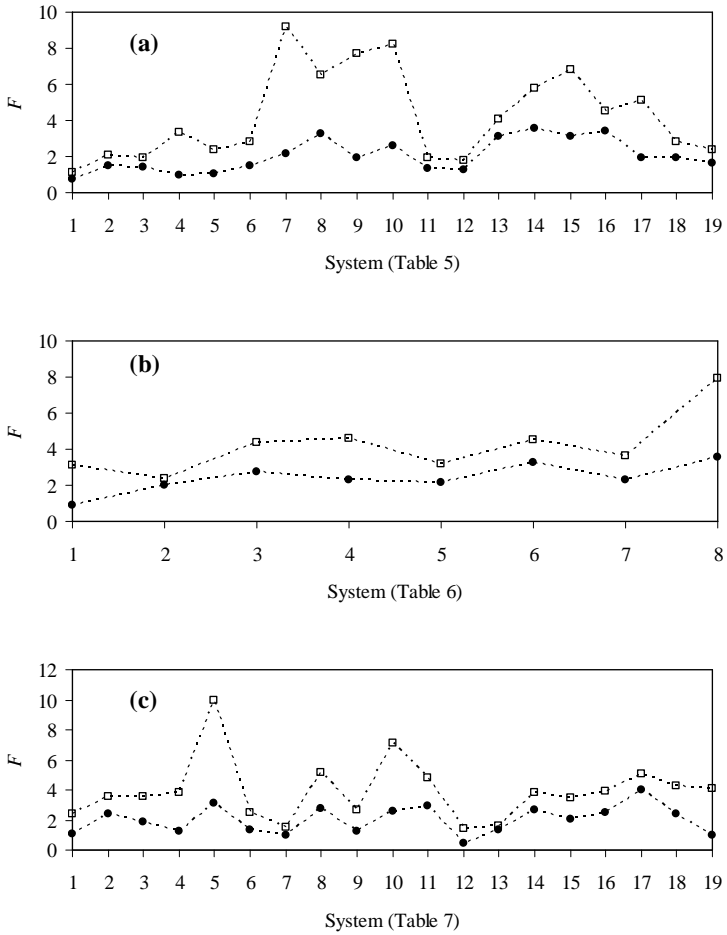


Figure 7. Inner behavior among the parameters of the PR-WS-VL model.

## 6. Conclusions

In this study, high-pressure vapor–liquid equilibrium data of binary mixtures containing supercritical fluids and imidazolium ionic liquids were correlated using a thermodynamic model optimized with a particle swarm algorithm. The Peng–Robinson (PR) equation of state the Wong–Sandler (WS) mixing rules including the van Laar (VL) model for the excess Gibbs free energy, were used as thermodynamic model. Forty-six binary systems taken from literature were selected for this study, and the optimization algorithm was used to determine the binary interaction parameters of each system. The algorithm was development to minimize the difference between calculated and experimental bubble pressure.

Based on the results and discussion presented in this study, the following main conclusions were derived: (i) PSO algorithm is appropriate to describe the vapor–liquid equilibrium of binary systems containing supercritical fluids and ionic liquids; (ii) the low



**Figure 8.** Comparison between PSO (●) and LM (□) optimizations used in the VLE modeling. (a) Systems at 313K, (b) systems at 323K, and (c) systems at 333K. In these figures, the systems are listed as in Table 5 to 7.

deviations obtained with the proposed PSO algorithm indicate that it can estimate the binary interaction parameters with better accuracy than other algorithms available in the literature; (iii) the values calculated with the PSO algorithm are believed to be accurate enough for engineering calculations, among other uses.

*Acknowledgments:* The author thank the Direction of Research of the University of La Serena (DIULS), and the Department of Physics of the University of La Serena (DFULS) for the special support that made possible the preparation of this paper.

## References

- [1] J. A. Lazzús, Estimation of density as a function of temperature and pressure for imidazolium-based ionic liquids using a multilayer net with particle swarm optimization, *Int. J. Thermophys.* **30** (2009) 883–909.
- [2] J. A. Lazzús, Hybrid particle swarm-ant colony algorithm to describe the phase equilibrium of systems containing supercritical fluids with ionic liquids, *Commun. Comput. Phys.* **14** (2013) 107–125.
- [3] A. Heintz, Recent developments in thermodynamics and thermophysics of non-aqueous mixtures containing ionic liquids: a review, *J. Chem. Thermodyn.* **35** (2005) 525–535.
- [4] T. Wang, C. Peng, H. Liu, Y. Hu, J. Jiang, Equation of state for the vapor-liquid equilibria of binary systems containing imidazolium-based ionic liquids, *Ind. Eng. Chem. Res.* **46** (2007) 4323–4329.
- [5] R. Kato, J. Gmehling, Measurement and correlation of vapor-liquid equilibria of binary systems containing the ionic liquids [EMIM][(CF<sub>3</sub>SO<sub>2</sub>)<sub>2</sub>N], [BMIM][(CF<sub>3</sub>SO<sub>2</sub>)<sub>2</sub>N], [MMIM][(CH<sub>3</sub>)<sub>2</sub>PO<sub>4</sub>] and oxygenated organic compounds respectively water, *Fluid Phase Equilib.* **231** (2005) 38–43.
- [6] L. A. Blanchard, D. Hancu, E. J. Beckman, J. F. Brennecke, Green processing using ionic liquids and CO<sub>2</sub>, *Nature* **399** (1999) 28–29.
- [7] J. A. Lazzús, J. Marín, Activity coefficient model to describe isothermal vapor-liquid equilibrium of binary systems containing ionic liquids, *J. Eng. Thermophys.* **19** (2010) 170–183.
- [8] A. Scurto, S. Aki, J. Brennecke, CO<sub>2</sub> as a separation switch for ionic liquid/organic mixtures, *J. Am. Chem. Soc.* **124** (2002) 10276–10277.
- [9] A. M. Scurto, S. N. V. K. Aki, J. F. Brennecke, Carbon dioxide induced separation of ionic liquids and water, *Chem. Commun.* **5** (2003) 572–573.

- [10] V. H. Álvarez, M. Aznar, Application of a thermodynamic consistency test to binary mixtures containing an ionic liquid, *Open Thermodyn. J.* **2** (2008) 25–38.
- [11] G. Hong, J. Jacquemin, M. Deetlefs, C. Hardacre, P. Husson, M. F. Costa Gomes, Solubility of carbon dioxide and ethane in three ionic liquids based on the bis{(trifluoromethyl)sulfonyl}imide anion, *Fluid Phase Equilib.* **257** (2007) 27–34.
- [12] R. Bogel-Lukasik, D. Matkowska, E. Bogel-Lukasik, T. Hofman, Isothermal vapor-liquid equilibria in the binary and ternary systems consisting of an ionic liquids, 1-propanol and CO<sub>2</sub>, *Fluid Phase Equilib.* **293** (2010) 168–174.
- [13] J. Yang, C. Peng, H. Liu, Y. Hu, Calculation of vapor-liquid and liquid-liquid phase equilibria for systems containing ionic liquids using a lattice model, *Ind. Eng. Chem. Res.* **45** (2006) 6811–6817.
- [14] J. A. Lazzús, Thermodynamic modelling based on particle swarm optimization to predict phase equilibrium of binary systems containing ionic liquids, *J. Mol. Liq.* **186** (2013) 44–51.
- [15] J. A. Lazzús, A. A. Pérez Ponce, L. Palma Chilla, Application of particle swarm optimization to model phase equilibrium of complex mixtures, *Fluid Phase Equilib.* **317** (2012) 132–139.
- [16] J. A. Lazzús, M. Rivera, Gas-solid phase equilibrium of biosubstances by two biological algorithms, *Rev. Mex. Fís.* **59** (2013) 577–583.
- [17] J. A. Lazzús, Optimization of activity coefficient models to describe vapor-liquid equilibrium of (alcohol + water) mixtures using a particle swarm algorithm, *Comput. Math. Appl.* **60** (2010) 2260–2269.
- [18] J. A. Lazzús, Optimization of a cubic equation of state and van der Waals mixing rules for modeling the phase behavior of complex mixtures, *Rev. Mex. Fís.* **58** (2012) 510–514.
- [19] J. Kennedy, R. C. Eberhart, Y. Shi, *Swarm Intelligence*, Academic Press, San Diego, 2001.
- [20] M. Schwaab, E. Chalbaud, J. L. Monteiro, J. C. Pinto, Nonlinear parameter estimation through particle swarm optimization, *Chem. Eng. Sci.* **63** (2008) 1542–1552.
- [21] V. H. Alvarez, R. Larico, Y. Ianos, M. Aznar, Parameter estimation for VLE calculation by global minimization: the genetic algorithm, *Braz. J. Chem. Eng.* **25** (2008) 409–418.
- [22] R. C. Eberhart, J. Kennedy, A new optimizer using particle swarm theory, in: T. Nishio, K. Ahe, N. Kato, H. Ota (Eds.), *Proceedings of the Sixth International Symposium on Micro Machine and Human Science*, IEEE, Piscataway, 1995, pp. 39–43.
- [23] Y. Jiang, T. Hu, C. C. Huang, X. Wu, An improved particle swarm optimization algorithm, *Appl. Math. Comput.* **193** (2007) 231–239.

- [24] Y. Da, G. Xiurun, An improved PSO-based ANN with simulated annealing technique, *Neurocomputing* **63** (2005) 527–533.
- [25] Y. Shi, R. C. Eberhart, A modified particle swarm optimizer, in: P. K. Simpson, D. B. Fogel (Eds.), *The 1998 IEEE International Conference on Evolutionary Computation Proceedings*, IEEE Press, Piscataway, 1998, pp. 69–73.
- [26] S. M. Walas, *Phase Equilibria in Chemical Engineering*, Butterworth, Storeham, 1985.
- [27] H. Orbey, S. I. Sandler, *Modeling Vapor–Liquid Equilibria. Cubic Equations of State and Their Mixing Rules*, Cambridge Univ. Press, Cambridge, 1998.
- [28] J. M. Prausnitz, R. N. Lichtenthaler, E. Gomes de Azevedo, *Molecular Thermodynamics of Fluid–Phase Equilibria*, Prentice Hall, New Jersey, 1999.
- [29] F. M. Maia, I. Tsivintzelis, O. Rodriguez, E. A. Macedo, G. M. Kontogeorgis, Equation of state modelling of system with ionic liquids: literature review and application with the cubic plus association (CPA) model, *Fluid Phase Equilib.* **332** (2012) 128–143.
- [30] D. Y. Peng, D. B. Robinson, A new two-constant equation of state, *Ind. Eng. Chem. Fundam.* **15** (1976) 59–64.
- [31] D. S. Wong, S. I. Sandler, A theoretically correct mixing rule for cubic equations of state, *AIChE J.* **38** (1992) 671–680.
- [32] P. Wasserscheid, T. Welton, *Ionic Liquids in Synthesis*, Wiley–VCH, Weinheim, 2008.
- [33] J. O. Valderrama, W. W. Sanga, J. A. Lazzús, Critical properties, normal boiling temperature, and acentric factor of another 200 ionic liquids, *Ind. Eng. Chem. Res.* **47** (2008) 1318–1330.
- [34] T. E. Daubert, R. P. Danner, H. M. Sibul, C. C. Stebbins, *Physical and Thermodynamic Properties of Pure Chemicals. Data Compilation*, Taylor & Francis, London, 1996.
- [35] A. Shariati, C. J. Peters, High–pressure phase equilibria of systems with ionic liquids, *J. Supercrit. Fluids* **25** (2003) 109–117.
- [36] A. Shariati, K. Gutkowski, C. J. Peters, Comparison of the phase behavior of some selected binary systems with ionic liquids, *AIChE J.* **51** (2005) 1532–1540.
- [37] P. J. Carvalho, V. H. Alvarez, J. J. B. Machado, J. Pauly, J. L. Daridon, I. M. Marrucho, M. Aznar, J. A. P. Coutinho, High pressure phase behavior of carbon dioxide in 1-alkyl-3-methylimidazolium bis(trifluoromethylsulfonyl)imide ionic liquids, *J. Supercrit. Fluids* **48** (2009) 99–107.
- [38] S. N. V. K. Aki, B. R. Mellein, E. M. Saurer, J. F. Brennecke, High–pressure phase behavior of carbon dioxide with imidazolium-based ionic liquids, *J. Phys. Chem.* **108B** (2004) 20355–20365.
- [39] L. A. Blanchard, Z. Gu, J. F. Brennecke, High–pressure phase behavior of ionic liquid/CO<sub>2</sub> systems, *J. Phys. Chem.* **105B** (2001) 2437–2444.

- [40] A. Pérez-Salado Kamps, D. Tuma, J. Xia, G. Maurer, Solubility of CO<sub>2</sub> in the ionic liquid [bmim][PF<sub>6</sub>], *J. Chem. Eng. Data* **48** (2003) 746–849.
- [41] P. Coutsikos, K. Magoulas, G. M. Kontogeorgis, Prediction of solid–gas equilibria with the Peng–Robinson equation of state, *J. Supercrit. Fluids* **25** (2003) 197–212.
- [42] M. A. Trebble, P. R. Bishnoi, Extension of the Trebble–Bishnoi equation of state to fluid mixtures, *Fluid Phase Equilib.* **40** (1988) 1–21.
- [43] M. Reilly, *Computer Programs for Chemical Engineering Education*, Sterling Swift, Manchaca, 1972.